IEEE Transactions on Plasma Science, Vol PS-5, No. 4, December 1977

NEW DEVELOPMENTS IN LASER DIAGNOSTICS FOR TOKAMAK PLASMAS

Francis F. Chen
School of Engineering and Applied Science
University of California
Los Angeles, California
Received November 5, 1976

ABSTRACT

New types of infrared and far-infrared lasers can be used to make otherwise impossible measurements of plasma parameters in the next generation of large tokamaks. Recent progress in the development of such new diagnostic techniques is reviewed.

I. INTRODUCTION

The major emphasis in fusion research in the United States, and probably also in the world, lies in the tokamak concept. Diagnostic techniques for the plasma in a tokamak are not completely satisfactory even at present and will become less satisfactory in the next generation of machines —— for example, the TFTR at Princeton and the T-20 in the USSR. Thomson scattering with ruby lasers can continue to be the principal diagnostic for electron temperature and density. Ion temperature is traditionally measured by the spectrum of charge exchange neutrals. In the new devices, which have a minor diameter of 1 m or more, this method cannot be used for the plasma interior because the neutrals have mean free paths shorter than the plasma radius. Spectroscopic analysis of impurity radiation in the ultraviolet is also difficult in large plasmas because of the relatively large impurity radiation from near the surface. There is as yet no good way to measure ion temperature in such devices.

The current distribution in a tokamak is important because it affects the radial variation of the safety parameter q and thus controls the hydrodyamic stability of the plasma. Measurement of the magnetic field direction would yield the current distribution as well as the observation of magnetic islands. Newly developed methods accomplish this by injection of neutral hydrogen or lithium beams——methods that also will fail in large diameter plasmas.

Another problem is that the usual method of measuring density and density variations--microwave interferometry--fails at densitites above about 5×10^{13} cm^{-3} because of the very large number of fringe shifts involved at microwave frequencies. Finally, one needs a method for measuring fluctuations in the plasma, so as to determine the importance of MHD modes, drift modes, and trapped particle instabilities on anomalous particle and heat transport.

In this paper, we review the progress in the development of diagnostics based on relatively new types of lasers. Topics treated are 1) Thomson scattering in the far infrared, 2) Measurement of poloidal field distributions, 3) Measurement of plasma fluctuations, and 4) Far-infrared interferometry.

II. REVIEW OF LASER SCATTERING

When an electron is placed in the electric field of a laser beam, it is accelerated and therefore emits radiation which can potentially be detected as scattered light. If the electrons in a plasma were uniformly spaced, however, their contributions would cancel, resulting in no net scattering. Because of density irregularities δn, either random or coherent, bunched electrons emit constructively an intensity proportional to $(\delta n)^2$. If δn is random, its magnitude varies as $n^{1/2}$; hence, scattered intensity from a thermal plasma is proportional to its density n. Scattering from a wave of amplitude $\delta n/n$ would have intensity $\propto (\delta n)^2$.

If the fluctuations have frequency ω and wavenumber $\underline{k}$, the scattered wave $(\omega_s, \underline{k}_s)$ is modulated by $(\omega, \underline{k})$ and hence satisfies the relations

$$\omega_s = \omega_o + \omega \qquad \underline{k}_s = \underline{k}_o + \underline{k}.$$

The scattering angle θ is defined by the following diagram:

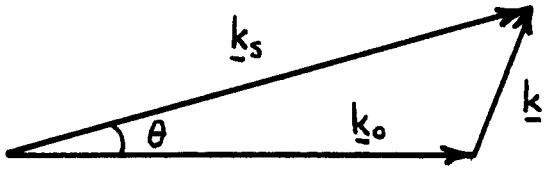

By choosing θ and ω_s (and hence $\underline{k}_s$), the experimenter can examine fluctuations of given ω and $\underline{k}$. If $|\,k\,|$ is chosen so that $k\lambda_D \ll 1$, the fluctuations have scale length larger than the Debye length and must therefore be cooperative plasma motions. If $k\lambda_D \gg 1$, the wavelengths being probed

are smaller than a Debye cloud and therefore relate to individual electron motions. It is customary to distinguish these two cases by the scattering parameter $\alpha \equiv (k\lambda_D)^{-1}$. For the usual case $|k_s| \simeq |k_o|$, the law of cosines gives

$$k^2 = k_o^2 + k_s^2 - 2k_o k_s \cos\theta \simeq$$

$$2k_o^2(1 - \cos\theta) = 4k_o^2 \sin^2 \tfrac{1}{2}\theta.$$

Thus

$$\alpha = (2k_o \lambda_D \sin \tfrac{1}{2}\theta)^{-1}. \qquad (1)$$

For $\alpha \ll 1$, the scattering is from individual electrons, which have a thermal velocity v_{th}. The Doppler shift $\omega = kv_{th}$, therefore, gives rise to a scattered spectrum whose width is indicative of the electron temperature T_e. For $\alpha \gg 1$, the scattering is from large-scale plasma motions, which could be unstable or induced waves or thermal fluctuations. In the absence of magnetic field $\underline{B}$, only two waves are possible: electron plasma waves and ion acoustic waves. These waves have a non-zero thermal level even in a quiescent plasma, and the scattered spectrum would have peaks near ω_p and $\omega_i = kc_s$, where c_s is the sound speed. Fig. 1 shows schematically the spectrum at different values of α.

The case $\alpha \ll 1$ corresponds to ordinary ruby laser scattering for measuring T_e. The case $\alpha \gg 1$ yields electron peaks near $\pm \omega_p$ which would give the density if there were not better ways to measure it. In addition, there is an ion peak whose shape depends on the temperature ratio T_e/T_i, as shown in Fig. 2. If $T_e/T_i > 1$, two peaks occur at $\pm kc_s$, since ion waves are not heavily Landau damped. The position of the peaks yields c_s, from which T_i can be calculated if T_e is known accurately. If $T_e/T_i < 1$, ion waves are Landau damped by the ions, and a single peak appears, whose width is related to T_i. In the intermediate case, the appearance of the flat-topped peak indicates that T_i is close to T_e. Thus ion temperature can be measured only if $\alpha \gtrsim 1$ can be achieved, and this means, from Eq. (1), either extreme forward scattering ($\theta \ll 1$) or long-wavelength lasers (small k_o).

If $B \neq 0$, many waves are possible, but the number can be narrowed down by proper choice of $\underline{k}$. For instance, if $\underline{k}$ is parallel to $\underline{B}$, only electromagnetic waves like Alfvén waves or whistlers are possible in addition to the two usual waves, but the latter will dominate because of their relatively small group velocities. On the other hand, if $\underline{k}$ is perpendicular to $\underline{B}$, new modes involving cyclotron or $\underline{E} \times \underline{B}$ motions arise which have no competition from $B = 0$ modes. Detection of such field-aligned fluctuations as drift waves or Bernstein modes would give information on the direction of $\underline{B}$. This method depends on $\alpha > 1$ scattering, which is difficult to achieve at angles θ large enough to give directional resolution. However, there is another method for $\alpha \ll 1$ which depends on individual electron motions. Since electrons gyrate at the cyclotron frequency

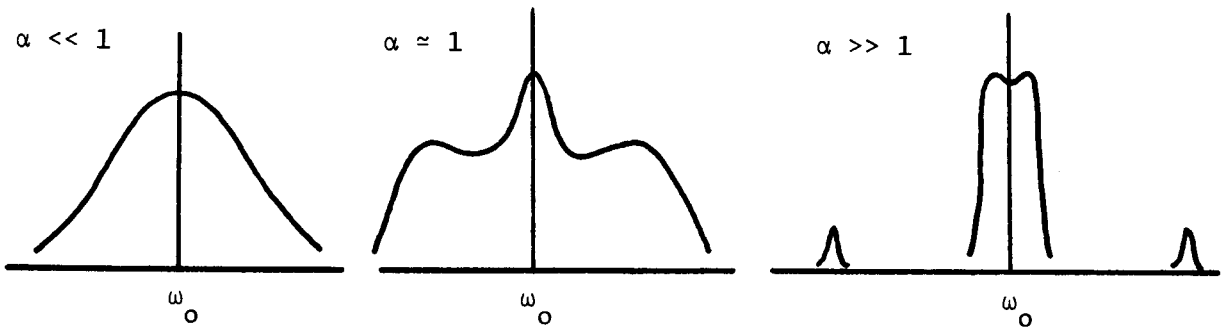

Figure 1.

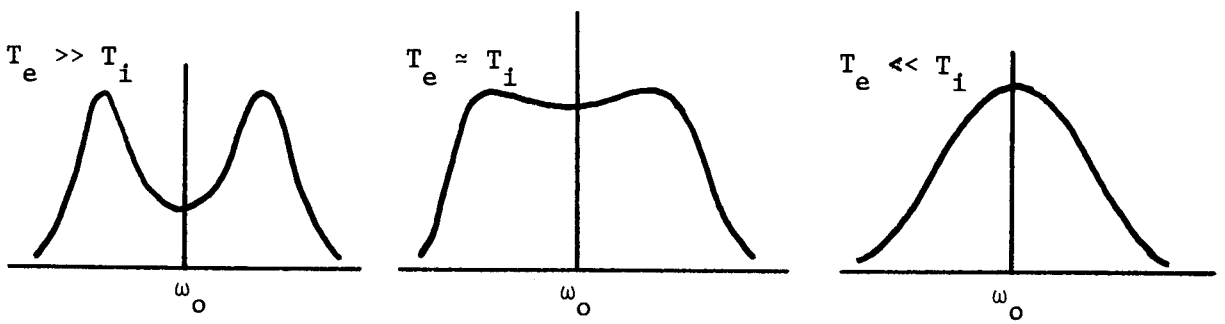

Figure 2.

ω_c regardless of velocity, light scattered from them has a Doppler shift $k_\perp v_\perp$ that varies in time at the frequency ω_c. This gives rise to a modulation of the spectrum of Fig. 1a. Although the total power remains the same, the spectrum is divided into peaks at harmonics of ω_c. These peaks would be smeared out, however, if the Doppler shifts $k_{\parallel} v_{\parallel}$ due to thermal motion parallel to B_o were as large as ω_c; thus, existence of the modulation means that $k_{\parallel} v_{\parallel} < \omega_c$, or that k is almost perpendicular to B_o. This is the basis of the field-direction measurement discussed in Sec. IV.

Since the Thomson cross section σ_T is very small (6.7×10^{-25} cm^2), only a few lasers have the requisite power, bandwidth, and reliability for scattering measurements. These are given in Table I.

TABLE I

Lasing medium	λ_o (μm)	Typical power	Typical pulse length
Ruby	0.69	1 GW	20 ns
Nd-glass	1.06	>> 1 GW	1 ns
CO_2 (TEA)	10.6	0.5 GW	50 ns
CH_3F	496	1 MW (projected)	50 ns

Although very large power is available with Nd-glass, this laser offers less than a factor-of-two improvement over ruby in λ_o and is comparatively inconvenient to use because the wavelength lies outside the visible. The CH_3F laser is representative of several molecular lasers in the 100-1000 μm range that can be pumped by CO_2 radiation.

In terms of tokamak parameters, Eq. (1) can be written

$$\alpha = 3.4 \times 10^{-3} \frac{\lambda_\mu}{\sin\frac{1}{2}\theta} \left(\frac{n_{14}}{T_{keV}}\right)^{\frac{1}{2}}, \qquad (2)$$

where λ_μ is λ_o in μm, n_{14} is n units of 10^{14} cm^{-3} and T_{keV} is T_e in keV. Thus, for $n \simeq 10^{14}$ cm^{-3} and $T_e \simeq 1$ keV, ruby lasers can be used for small-α scattering only, while CO_2 lasers can be used for large-α scattering only at extreme forward angles. Far-infrared lasers have the capability of giving ion temperature information at large α even if $\theta = 90°$. The range of n and T_e covered by various lasers at various θ are shown in Fig. 3.

III. MEASUREMENT OF T_i BY LARGE-α SCATTERING

There are basically only two ways to do Thomson scattering at $\alpha \sim 1$ to measure ion temperature under tokamak conditions: forward scattering at 10.6 μm and large-angle scattering in the far-infrared. Detection of forward-scattered CO_2 radiation at $\theta = 6° - 8°$ has been

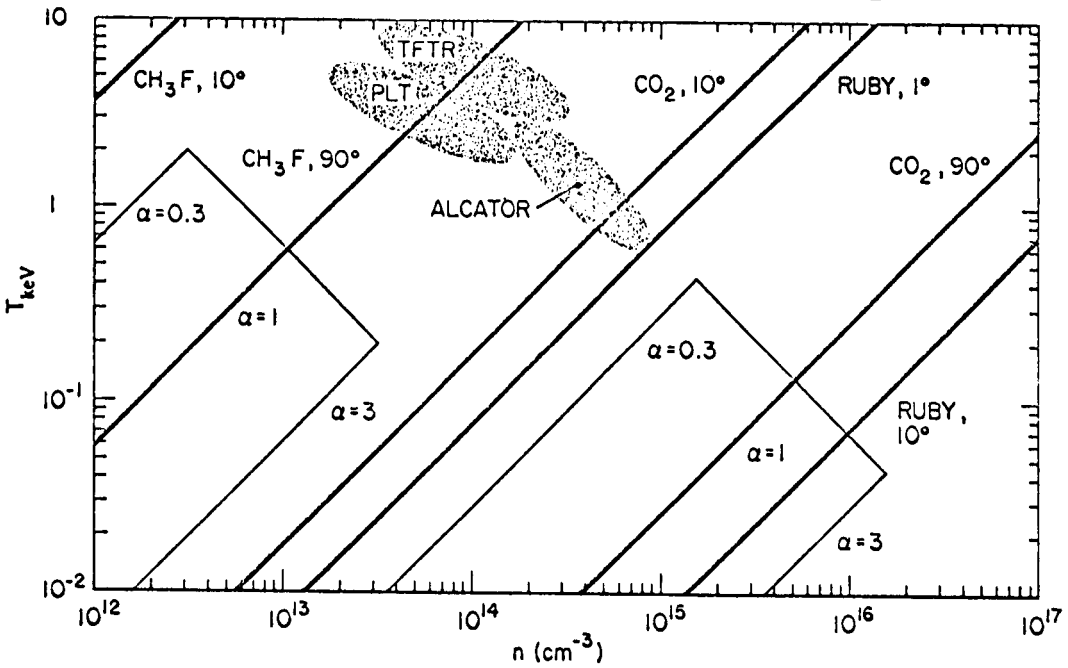

Figure 3. Range of plasma parameters covered by various lasers and scattering angles. Heavy lines indicate $\alpha = 1$, light lines show the effect of changing α by half an order of magnitude. Expected range of the PLT and TFTR tokamaks at Princeton is shown, together with that of a projected high density Alcator at M. I. T.

achieved with ordinary-bandwidth ($\simeq$ 1 GHz FWHM) TEA lasers applied to pinch plasmas. Bretz and De Silva [1] used a θ-pinch with $n = 1.6 \times 10^{13}$ cm^{-3} and $T_e = 0.5$ eV, while Craig et al. [2] used a z-pinch with $n = 6 \times 10^{14}$ cm^{-3} and $T_e = 1.2$ eV and obtained frequency resolution at the higher density. In both cases detection was successful only because the fluctuation level was $10^2 - 10^3$ times higher than thermal.

To improve the detection sensitivity and lower the scattering angle, Gondhalekar and Keilmann [3] proposed a baffle system, shown in Fig. 4, and homodyne detection, which makes use of stray light as a local oscillator. Successful tests of homodyne detection were made by two groups: Gondhalekar and Holzhauer [4] and Baker, Heckenberg, and Meyer [5]. The former used an arc plasma with $n = 10^{15}$ cm^{-3} and $T_e = 4$ eV, and the heterodyne signal at $\theta = 1.8^o$ showed the presence of 20 MHz oscillations at a level well above thermal. The latter observed scattering from externally generated 4.5–MHz ion waves at $\theta = 1^o$ and a density of only 10^{12} cm^{-3}. Other heterodyne experiments will be discussed in Section V.

In homodyne or heterodyne detection, the laser must have high mode purity and a bandwidth much less than the width of the ion peak in the scattered spectrum. These requirements are met by the hybrid laser [6], which comprises two separate discharges in the same optical cavity: a high pressure discharge to supply the power, and a low-pressure discharge to determine the mode. The latter is designed so that only a single longitudinal mode lies within the 60 MHz Doppler-broadened line profile. Typically [4], a pulse of 80 kW for 1.8 μsec can be obtained with adjacent-mode rejection of 10^9. Although 300 kW powers have been reported [6] for the hybrid laser, tokamak diagnostics would require an order of magnitude higher power [3]. Perhaps the method of injection [7] could be developed to produce pulses of requisite length and purity.

Another requirement is that the detector have sufficient bandwidth. The half-width of the ion peak for $T_i \simeq T_e$ is given approximately by

$$\omega = kc_s = 2k_o \sin\tfrac{1}{2}\theta (8KT/3M)^{\frac{1}{2}} \qquad (3)$$

For $\theta = 1^o$ in a 1 keV hydrogen plasma, this amounts to 0.8 GHz for CO_2. State-of-the-art photoconductor detectors can be made with 1 GHz bandwidth and requisite sensitivity [8], but an optimized detection system is quite costly and has not yet been tested in such an application. In the experiments referred to above [4,5], only 100 MHz bandwidth was available. At larger scattering angles than 1^o or higher temperatures than 1 keV, bandwidth becomes a limiting factor. Fortunately, the large local oscillator power in heterodyne detection lowers the detector resistance and makes the design of the detector circuitry easier.

Forward scattering suffers from the lack of spatial resolution; the depth of focus defines a long scattering volume, giving rise to a range of scattering angles θ. Straightforward detection, as is being attempted at Culham, requires very large laser power ($>$ 1 GW) and meticulous reduction of stray light, but not the spectral purity, long pulse length, and detector frequency response needed in homodyne detection. The latter demonstrably works with coherent fluctuations, but the data from the purely random fluctuations of a thermal plasma may be hard to interpret. Finally, the CO_2 wavelength does not allow much flexibility in the choice of α over a large range of plasma parameters.

These problems are overcome if one uses a far-infrared (FIR) laser, but this technique is not as well developed. We consider, for example, large-angle Thomson scattering with a 496-μm CH_3F laser with heterodyne detection using a dc far-infrared laser as a local oscillator and a Schottky-barrier diode as a detector-mixer. Assuming that a power P_o of about 2 MW will be available and that the scattered power can all be focussed onto the detector, the numbers come out about the same as for the CO_2 homodyne case discussed above. The scattered power P_s is given by

$$P_s = P_o n_e \sigma_e S(\alpha)\, \ell\, d\Omega, \qquad (4)$$

which does not depend on λ_o. The differential Thomson cross section σ_e depends weakly on θ, and the form factor $S(\alpha)$ is insensitive to α at large α. For reasonable values of the geometrical factors ℓ (length of the scattering volume) and $d\Omega$ (solid angle seen by the detector), P_s for $n_e = 10^{14}$ cm^{-3} is of order 10^{-8} W in both the CO_2 and CH_3F cases [3,9]. Reported heterodyne sensitivities are 8×10^{-20}

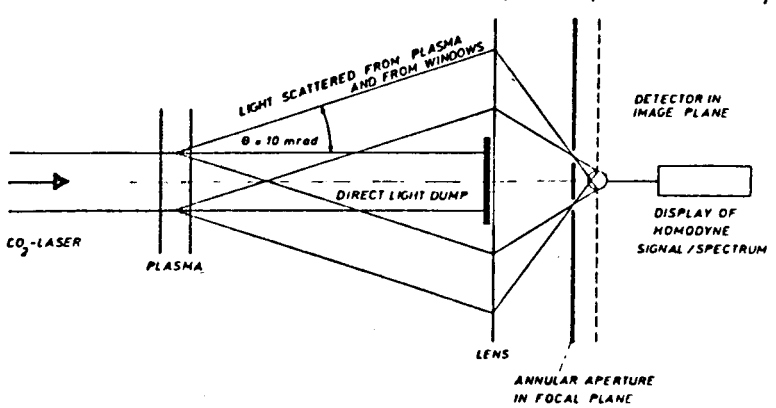

Figure 4. CO_2 forward scattering system proposed by Gondalhekar and Keilmann (Ref. 3).

W/Hz for CO_2 (Ge:Cu at 4.2° K, 100 mW local oscillator power [8]) and 10^{-17} W/Hz for FIR (GaAs Schottky diode, 10 mW local oscillator [10]). For a 1-GHz bandwidth, therefore, adequate detectors exist for CO_2 but need further development for FIR. Improvement by at least an order of magnitude is quite likely, since higher-power FIR oscillators are now becoming available.

The advantage of an FIR wavelength lies in the ability to achieve $a > 1$ at large scattering angle θ. At $\theta = 90°$, the scattering volume is clearly defined by the collection optics, and, more important, stray light can be reduced to a very low level. It is then possible to heterodyne with a separate oscillator rather than homodyne with the stray light, as one is forced to do in forward scattering. Since the dc oscillator can be made to give a single, narrow line, the requirements on mode purity of the primary laser can be relaxed without fear that a complicated pattern of beat frequencies will be superimposed on the scattered signal. A wide choice of available FIR laser lines should allow the IF frequency to fall in a convenient range for conventional microwave equipment.

These potential advantages of FIR scattering, of course, cannot be realized without a narrow-line laser of adequate power; and up to now the development of such a laser has taken top priority. Megawatts of power have been achieved with a superradiant D_2O and CH_3F systems, but with too large a bandwidth. Pulsed HCN lasers at 337 μm have been tried at Culham and at UCLA, but without success above 1 kW. Optical pumping of CH_3F by the 9.55 μm line of a CO_2 laser is a promising method being followed in several laboratories [11-15]. In these papers, powers in the 100-250 kW range at 496 μm wavelength with bandwidth 30-60 MHz were reported. This bandwidth is comparable to that obtainable with hybrid CO_2 lasers, so that neither method has an advantage as long as a, and hence, the width of the scattered spectrum, is constant. The various CH_3F experiments are all oscillator-amplifier systems and differ in the way the CO_2 power is coupled into the FIR amplifier.

Perhaps the cleverest scheme is that used by Semet and Luhmann [14], shown in Fig. 5. This scheme takes advantage of the fact that the FIR output is cross-polarized relative to the CO_2 pump, for the following reason. The CH_3F molecule is long, say, in the horizontal direction, with a methyl group at one end and a fluorine atom at the other. The 9.55 μm pump transition changes the vibrational state and is best excited by horizontally polarized light. The lasing transition, however, takes place between two rotational states; hence, the 496-μm radiation is emitted in a vertical plane. In Fig. 5, the output from a grating-controlled transverse-discharge CO_2 oscillator is split so that 80% of it is used to pump the FIR oscillator, entering it through a Ge plate and a Si etalon, which is also the output coupler for the FIR. The rest of the CO_2 power is amplified by a chain of TEA modules and then sent through the Ge plate into the FIR amplifier. The Ge plate is at the Brewster angle for both CO_2 beams. Since the FIR output is polarized at right angles, it is reflected from the Ge plate and also enters the FIR amplifier, which is simply a long Cu tube serving as a metallic waveguide. A dielectric wall is used to suppress high-order modes in the FIR oscillator, and this controls the bandwidth of the amplified pulse. Timing between the two CO_2 pumps is adjusted by time-of-flight. It was shown in this experiment that a conversion efficiency of 0.1% from 9.55-μm power to 496-μm power could be maintained for low powers up to nearly 200 kW by proper adjustment of the CH_3F pressure and the pump timing. Some improvement in this figure can be expected, since the theoretical efficiency is 1%, and 0.47% has been reported at the 6 kW level [12]. Even without improve-

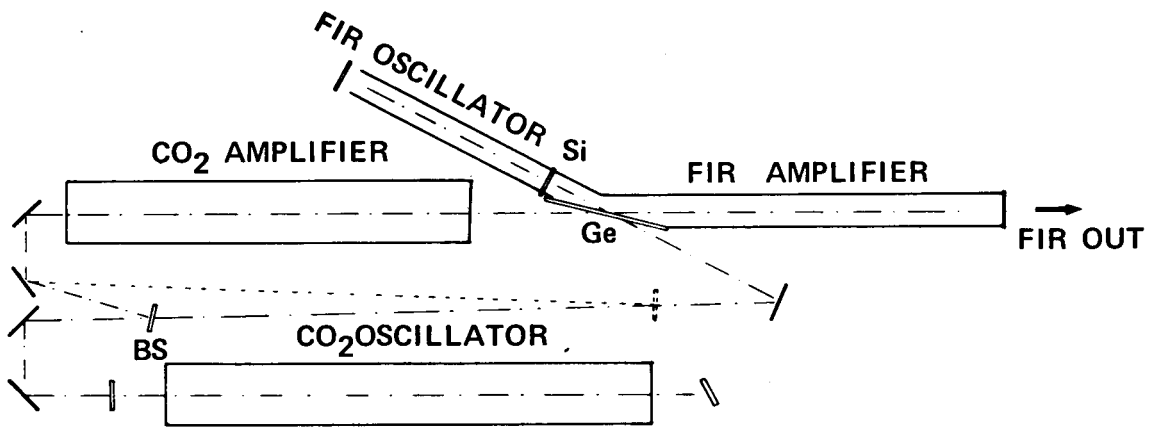

Figure 5. Experimental arrangement for optically pumped CH_3F laser (Semet and Luhmann, Ref. 14).

ment, straightforward application of 2 GW of CO_2 power would be expected to produce 2 MW at the desired frequency. The metallic waveguide offers an easy way to transport the beam into a tokamak.

Besides the detector threshold, the scattered power must also overcome the background of synchrotron radiation. At 50 kG, 496 μm corresponds to about the fourth harmonic of ω_c and hence lies well within the frequency range of synchrotron radiation. At 50 kG, 10^{14} cm^{-3} and T_e = 2 keV, the latter amounts to 0.3 W/cm^3 over the entire volume of plasma seen by the detection optics. Fortunately, the radiation is heavily reabsorbed, and what is seen is the black body radiation from the surface of the plasma. If the collecting lens is about 1 m from this surface, it will see about 5 cm^2 of plasma surface and cover about 2×10^{-3} steradians. For a 1-GHz bandwidth, the synchrotron power is then $\simeq 10^{-6}$ W, about two orders of magnitude larger than the scattered power. However, this is a dc background which can be distinguished from the laser pulse, and only fluctuations in the synchrotron radiation are troublesome. Nonetheless, this effect is one of the major uncertainities in this diagnostic.

Since laser powers perhaps as high as 10 MW will be needed to overcome the radiation background, one must be sure that the laser does not heat the electrons, since α depends on T_e/T_i. We assume the worst case——no heat conduction——and consider classical absorption of a 50-nsec pulse from either a 1-GW CO_2 laser focussed to 1 mm^2 or a 5-MW CH_3F laser focussed to 10 mm^2. In both cases the fractional temperature change is

$$\frac{\Delta T_e}{T_e} = 5 \times 10^{-3}\, n_{14}/T_{keV}^{5/2}, \qquad (5)$$

and heating does not appear to be a problem. This calculation, however, includes only collisional absorption and not synchrotron absorption. It is clear that the laser frequency must be above the lower harmonics of ω_c, where the latter effect is large. From this standpoint, it would be desirable to develop shorter wavelength lasers such as D_2O.

We next consider refraction, which may misalign the focal spot relative to the collection optics. In the limit of geometrical optics, if a ray is incident, with an impact parameter r_o, on a cylindrical plasma with a parabolic density profile, it will be refracted away from the axis and have a distance of closest approach to the axis equal to $r_{min} = r_o + \Delta r$. The maximum Δr as r_o is varied is an estimate of the amount of misalignment possible. Thus turns out to be

$$\Delta r = 0.19a\, n_o/n_c, \qquad n_c \equiv m\omega_o^2/4\pi e^2, \qquad (6)$$

where a is the plasma radius. For a = 100 cm and CO_2, Δr is 2 μm, which is negligible. For CH_3F, it is 4 mm, which is appreciable.

In large-α scattering with either CO_2 or CH_3F, one is likely to encounter suprathermal fluctuations. Although this enhances the detectability of the scattered light, ion temperatures cannot be measured in the canonical manner; rather, they must be deduced from the dispersion of the wave motions. If the difference $\underline{k}$ is perpendicular to $\underline{B}$, the waves are not likely to be sensitive to T_i; but if one chooses $\underline{k}$ parallel to $\underline{B}$ with $|k\lambda_o| < 1$, ion waves should be seen whose velocity depends on T_i. Because of the placement of ports in a tokamak, it is not easy to set $k \| B$ except in forward scattering. Consequently, with CH_3F the experiment would have to be done at very large α. If one does this (forward scattering at 496 μm), one may find a peak in the scattered light when $\underline{k}$ is nearly perpendicular to $\underline{B}$, corresponding to drift-type waves with $|k\lambda_D| \ll 1$ and $k_\parallel \ll k_\perp$. This could be an alternate method for determining the direction of $\underline{B}$.

IV. MEASUREMENT OF THE DIRECTION OF $\underline{B}$

The ω_c-modulation of the $\alpha \ll 1$ spectrum at $\theta = 90^o$, discussed physically in Sec. II, was calculated long ago by Salpeter [16] and has been seen in ruby scattering from high-density plasmas by Kellerer [17] and by Evans and Carolan [18,19]. Application to tokamaks using ruby lasers was suggested by Sheffield [20], and using CO_2 lasers by Murakami and Clarke [21], Perkins [22], and Bretz [23]. Figure 6 shows the configurations of various vectors at $\theta \simeq 90^o$. Let $\underline{k}_o$ be perpendicular to the total field $\underline{B}$, consisting of a strong toroidal component $\underline{B}_t$ and a weak poloidal component $\underline{B}_p$. This is the case if the incident laser beam is directed at the minor axis of a tokamak plasma. (If it is directed at the major axis as well, the system will be less sensitive to shifts of the plasma column in the azimuthal plane [21].) Let θ be the angle between $\underline{k}_o$ and $\underline{k}_s$, as usual. The difference vector $\underline{k}$ lies in the plane of $\underline{k}_o$ and $\underline{k}_s$, which makes an angle ϕ with the plane perpendicular to $\underline{B}$. If the scattering plane is rotated so that the two planes coincide (ϕ = 0), the ω_c-modulation will reach its maximum amplitude.

The laser power required is larger than for large-α scattering, not because any of the factors in Eq. (4) is greatly changed, but because homodyne detection is not possible. For fields above 1 kG, the cyclotron fundamental is about 2.8 GHz, and there are no detectors with sufficient bandwidth. Hence, laser powers of 1 GW or above are generally required, giving scattered powers of order 10^{-7} W. Fortunately, heating of the plasma by the laser does not directly affect this measurement, which consists of finding a maximum in the modulation of the spectrum as the

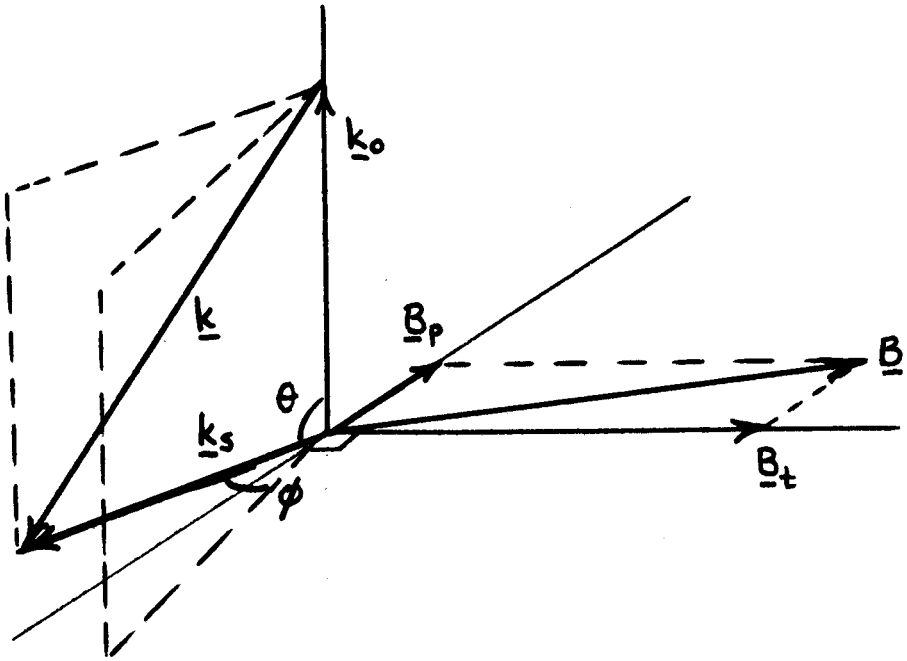

Figure 6. Geometry of 90° scattering in a magnetic field.

angle ϕ between k and the normal to B is varied. Both ruby and atmospheric-pressure CO_2 lasers have sufficient power and narrow enough bandwidth to resolve the cyclotron harmonics. Ruby has a great advantage in detection, since photomultipliers and image intensifiers can be used. However, there is a problem with quantum statistics. The choice between ruby and CO_2 depends on several conflicting requirements.

First, α should be $\ll 1$, since the effect depends on the incoherent motion of electrons. This can easily be satisfied with either laser, as seen in Fig. 3. Note, however, that cyclotron harmonics would occur even if $\alpha > 1$ because of Bernstein modes; one merely loses intensity by the factor $S(\alpha) = (1 + \alpha^2)^{-1}$.

Second, Doppler shifts due to thermal motion along B would smear out the modulation if $k_{\parallel} v_{th} > \omega_c$, where $k_{\parallel} = k\sin\phi$. Thus, for $\phi \ll 1$, the critical value of ϕ is

$$\phi_c = \omega_c / k v_{th}. \tag{7}$$

Since $\alpha = (k\lambda_D)^{-1}$, the angular resolution is given roughly by

$$\phi_c = \omega_c \alpha \lambda_D / v_{th} \simeq (\omega_c/\omega_p)\alpha \tag{8}$$

The resolution required is $\phi \ll B_p/B_t$, the pitch angle of the lines of force. In terms of the tokamak parameter $q = rB_t/RB_p$, we require $\phi \ll r/Rq$. For a tokamak with aspect ratio 3 with $q = 4$ at the edge, $r = a$, this gives $\phi \ll 4.8^o$. If measurements down to $q = 1$ at $r = a/4$ are required, we need $\phi \ll 3.6^\circ$. Thus, $\theta < 1/2 - 1^\circ$ [or $0.5 - 1^\circ$] should suffice. Assuming $\theta = 10^{-2}$ rad, and that $\omega_c/\omega_p \sim 1$, as it is in reactors and advanced tokamaks, we see from Eq. (8) that $\alpha < .01$. This is easily achieved with ruby but is marginal with CO_2.

Finally, we consider the number of photons in each peak— a number that cannot be too small if the observation of the modulation is to be statistically significant. An example given by Sheffield [20] for a 10 J ruby laser and $B = 25$ kG, $n = 2 \times 10^{13}$ cm^{-3}, $T_e = 900$ eV showed that the spectrum is divided into 10^2 cyclotron peaks and that only about 3 photoelectrons would appear in each peak for a reasonable detector system. The number of photons in each peak can be estimated as follows. The scattered energy, from Eq. (4), is

$$W_s = W_o n_e \sigma_e S(\alpha)\ \ell\ d\Omega \tag{9}$$

If each photon has energy $h\upsilon$, the number of photons is $W_s/h\upsilon$. The number of peaks is the width of the spectrum, $2k_{\perp}v_{th}$, divided by ω_c; hence the average number of photons in each peak is

$$N = \frac{W_o n_e \sigma_e\ \ell\ d\Omega}{h\nu}\ \frac{\omega_c}{2kv_{th}}, \tag{10}$$

where $k \sim k_{\perp}$ for small ϕ, and $S(\alpha) = 1$ for small α. The solid angle $d\Omega$ is $d\theta d\phi$ (cf. Fig. 6). There is no restriction on the range $d\theta$ covered by the collecting lens, but $d\phi$

is limited to $2\phi_c = 2\omega_c/kv_{th}$. (Actually, Carolan and Evans [19] showed that $d\phi$ can be considerably larger than this if the different rays collected by a finite lens are properly averaged.) We therefore have [17]

$$N \propto \frac{W_o}{h\nu}\left(\frac{\omega_c}{kv_{th}}\right)^2 \simeq \frac{W_o}{h\nu}\left(\frac{\alpha\omega_c}{\omega_p}\right)^2. \qquad (11)$$

If W_o and α are kept constant, there are more photons per peak for CO_2 than for ruby simply because the quanta are smaller by the ratio of wavelengths——15. If θ is kept constant instead of α, CO_2 has an additional advantage because the width of the spectrum, $4k_o v_{th} \sin 1/2\theta$, [or $4k_o v_{th} \sin(\theta\text{-}2)$], is smaller; and the energy is divided into fewer peaks. From this consideration, the value of α should be as large as the required angular resolution will allow - about 10^{-2} under tokamak conditions. For ruby, this would mean forward scattering, with the concomitant problems or poor spatial resolution and copious stray light. Whether ruby or CO_2 on better is balance is not clear at the moment.

A clever method has been suggested [20,23] to increase the detected signal. This is to use a Fabry-Perot interferometer with a plate spacing adjusted so that its free spectral range corresponds to ω_c. Fig. 7 shows the modulated spectrum, collected by a finite lens subtending a half-angle $\phi = 0.85^o$. Below it is the well-known transmission of a Fabry-Perot interferometer. Both the free spectral range and the finesse of the Fabry-Perot can be adjusted to match the expected spectrum. Thus, the energy in all the peaks is summed. As the interferometer is scanned, the signal transmitted to the detector will vary if the spectrum is modulated but will remain constant if it is not. Alternatively, we can suppress the stray light at $\omega = 0$ at the expense of half the energy by using a spacing of $2\omega_c$, as shown in Fig. 7c. Note that the spacing is set by the stronger component B_t, which is constant.

Sources of background radiation are bremsstrahlung or line radiation, synchrotron radiation, and 300°K blackbody radiation from the vacuum chamber and detector housing. The latter is peaked near the CO_2 laser frequency but can be lowered by cooled baffles. In any case, it is constant with time. Synchrotron radiation should be much less severe than in the FIR scattering case, because of the higher laser frequency and power. Other plasma radiation can be discriminated against by the fast rise of the laser signal. For this reason, the detector must have wide bandwidth even if heterodyning is not possible here.

A test of the feasibility of the CO_2 scheme is being carried out at UCLA by W. A. Peebles, M. J. Herbst, and J. J. Turechek. Their apparatus is shown in Fig. 8. The plasma is a laser-heated arc with $n \simeq 10^{15}$ cm^{-3}, $T_e \simeq$ 100 eV, and B = 4 kG. The laser is an 0.5 GW TEA CO_2 system. In this experiment, α is $\simeq 0.25$ and $\phi_c \simeq 0.6^o$.

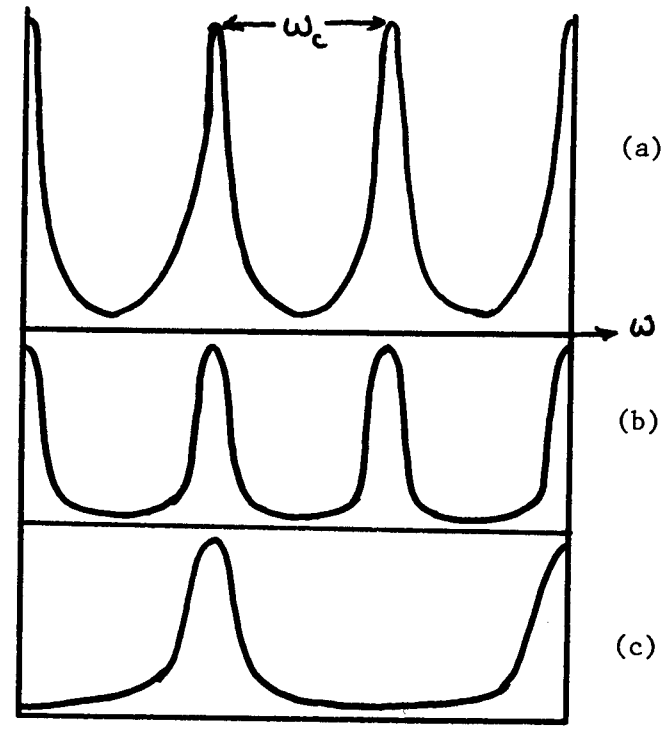

Figure 7. Cyclotron-modulated spectrum when k is perpendicular to B (from Carolan and Evans, Ref. 19).
(a) (b) Transmission of Fabry-Perot interferometer with free spectral range = ω_c.
(c) Same with half the plate spacing.

The light transmitted through and reflected from the Fabry-Perot interferometer is detected with separate photoconductors. A difference between their signals would indicate modulation. Stray light has been the main obstacle so far; background radiation does not appear serious. However, it was found that Ge:Hg detectors do not perform well without a local oscillator signal because of the high impedance of the poorly illuminated parts of the crystal. Besides this experiment, tokamak tests are being made with a ruby laser at Culham and with a CO_2 laser at Princeton [23]. No results have yet been reported, and the feasibility of this diagnostic is still unknown.

V. HOMODYNE DETECTION OF FLUCTUATIONS

The basis for large-α homodyne detection of plasma waves has already been discussed in Sec. III. Successful observation of beat frequencies using forward scattering with CO_2 hybrid lasers has been reported by two groups [4,5]. In those experiments, the pulse length was of the order of microseconds, restricting the observable frequencies to the range above 1 MHz. Furthermore, scattering angles $\geq 1^o$ were used, restricting the range of

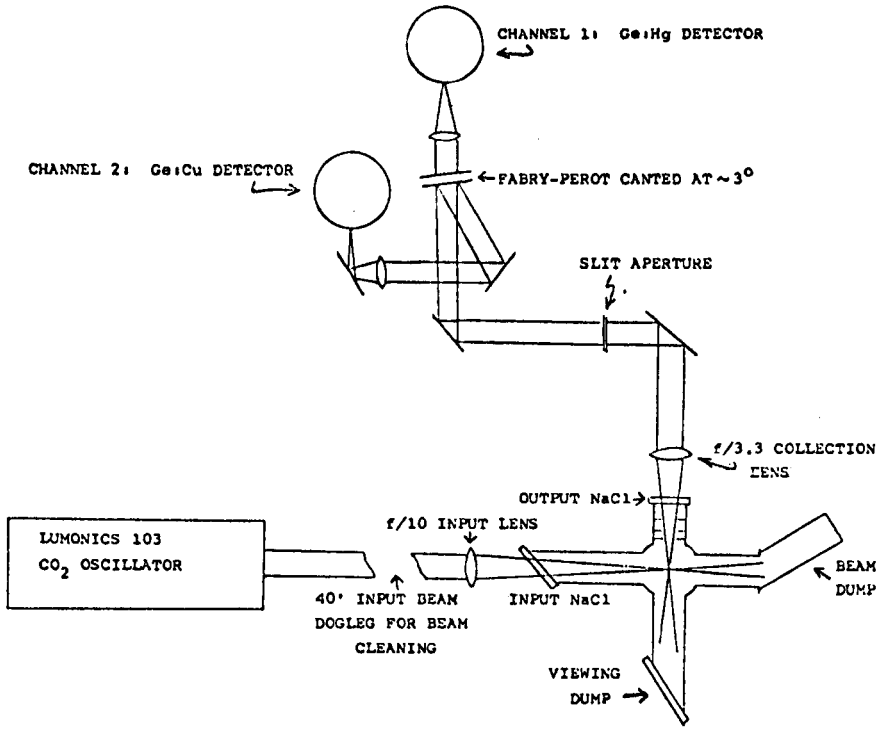

Figure 8. UCLA experiment to test field-direction measurement with CO_2.

wavelengths to below 0.06 cm, according to the relation $\lambda = 1/2\lambda_0/\sin 1/2\theta$ [or $\lambda = \lambda_0/2\sin(\theta\text{-}2)$]. Although such fine-scale fluctuations could, in principle, cause anomalous electron heat transfer, low-frequency drift-type oscillations are likely to be more dangerous in long-confinement-time devices, since they can cause partial transport of both species. To observe such oscillations requires long-pulsed lasers and scattering angles as small as 1 mrad (.06°), corresponding to λ = 1 cm with CO_2. Two groups have developed the equipment necessary for this type of measurement.

Slusher et al. [24] have succeeded in obtaining a two-dimensional map of the k spectrum of current-driven ion acoustic turbulence generated in a positive column, using a 400-W dc CO_2 laser and a 1-GHz Ge:Cu detector. Scattering angle was 0.6°, and measured fluctuations lay in the λ = .03–0.2 cm, f = 10–30 MHz range. This technique was then applied to the ATC tokamak at Princeton [25]. The frequency spectrum of oscillations between 0.1 and 2 MHz and the $\underline{k}$ spectrum between λ = 0.5 mm and = 2 cm have been measured in each of two directions. The fluctuation level was $\tilde{n}/n_0 \simeq 10^{-2}$, but in principle a sensitivity of $\tilde{n}/n_0 = 10^{-6}$ is supposed to be possible for $\lambda \leq 1$ mm. This tool is particularly useful is diagnosing the details of rf heating; however, a search for 800-MHz lower-hybrid heating waves at the $\tilde{n}/n_0 = 10^{-2}$ level has not given a detectable signal.

Lovberg [26] has taken a slightly different approach. Instead of a dc laser, he has developed a long-pulse CO_2 pin-laser with Cassegrain optics (Fig. 9). This produces a constant power level of 4 kW for 0.6 msec. The beam is carefully apodized so that a scattering angle of 0.17° can be achieved in homodyning. The system is to be applied to a tokamak (the UCLA Microtor) using only one window (Fig. 10).

VI. FAR-INFRARED INTERFEROMETRY

Microwave interferometry in the 2-8mm wavelength range has been a standard diagnostic to monitor the density pulse in toroidal devices. From the dispersion relation

$$\frac{c^2k^2}{\omega^2} = 1 - \frac{\omega_p^2}{\omega^2}, \quad k = \frac{\omega}{c}\left(1 - \frac{\omega_p^2}{\omega^2}\right)^{1/2} \tag{12}$$

one finds that the phase shift across a plasma of diameter L is

$$\Phi = \int_0^L (k_0 - k)\,dz \simeq$$

$$k_0 L\left[1 - \left(1 - \frac{\omega_p^2}{\omega^2}\right)^{1/2}\right] \simeq \tfrac{1}{2}\frac{\omega_p^2 L}{c\omega}. \tag{13}$$

As tokamak dimensions become large, Φ becomes inconveniently large unless ω is increased. Furthermore, as the

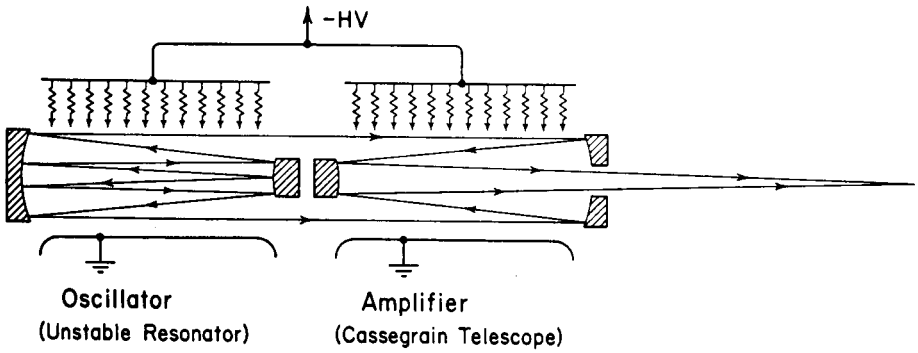

Figure 9. Specially designed long-pulse CO_2 laser-amplifier system for homodyne detection of fluctuations (Lovberg).

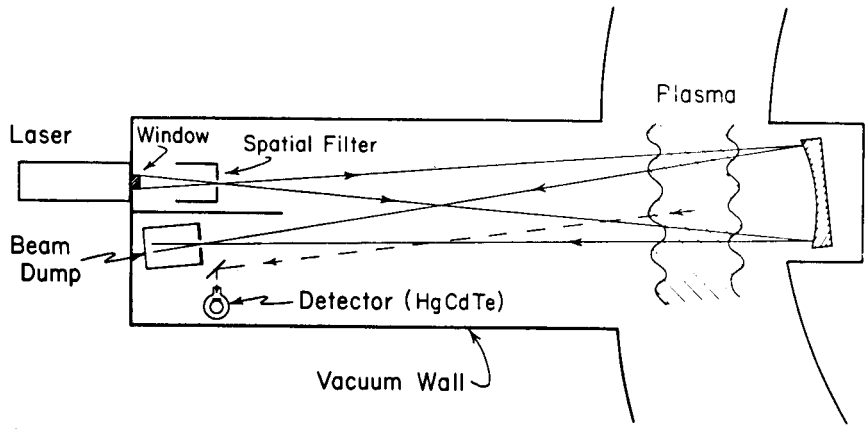

Figure 10. Experimental arrangement for tokamak scattering experiment (Lovberg).

density approaches the critical density, refraction and absorption become important, and the nonlinearity of Eq. (12) becomes inconvenient. Interferometers in the far infrared solves this problem. For many years, it has been possible to produce 10's of mW of dc power at 337 μm with the HCN laser [27]. The HCN laser, however, requires considerable maintenance, since the walls and internal optics have to be cleaned periodically of deposits made by the discharge.

Recent progress in optical pumping with dc CO_2 lasers has made more compact and reliable FIR waveguide lasers available. A list is given in Table II.

A particularly well engineered interferometer based on the 118-μm alcohol laser has been developed by M. I. T. group [29]. A diagram of it is shown in Fig. 11. To achieve the "zebra" display usually employed in microwave interferometry, two 5-mW alcohol lasers are set to a frequency difference of 1 MHz $\pm$ 2% by a feedback system on the mirrors, with the correction signal derived from the first set of beam splitters. The beams are then used as the probe and reference beams, and the 1-MHz modulation provides the sweep needed for the zebra display.

TABLE II [27]

Molecule	Wavelength (μm)	Laser length (m)	Pump power (W)	FIR power (mW)
CH_3OH	118	1	27	150
CH_3OH	118	2	60	400
CH_3OH	71	1	30	100
CH_3F	496	1	30	22
CH_3F	496	2	60	40

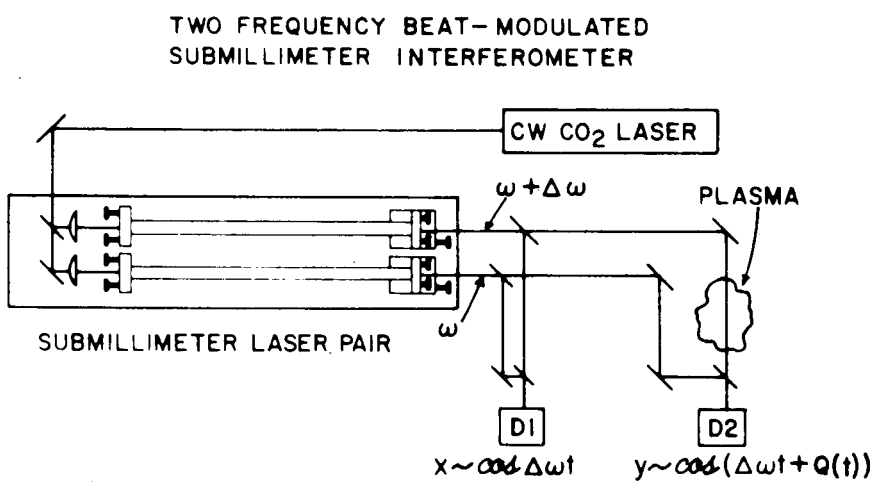

Figure 11. Alcohol-laser interferometer developed by M. I. T. (Ref. 29).

Other FIR diagnostics such as refraction and schlieren refractometry are in principle possible, but we know of no new developments in this area.

VII. ACKNOWLEDGEMENTS

The author is indebted to his collegues N. C. Luhmann, Jr., W. A. Peebles, and J. J. Turechek for instructive discussions and access to unpublished data. He is also grateful to many of the authors whose work is referred to here, who have given permission to quote their results, published or unpublished. This work was supported by the U. S. Energy Research and Development Administration, Contract E(11-1) Gen. 10, P. A. 26.

REFERENCES

1. N. L. Bretz and A. W. DeSilva, *Phys. Rev. Letters* **32**, 138 (1974).
2. A. D. Craig, S. Nakai, D. D. R. Summers, and J. W. M. Paul, *Phys. Rev. Letters* **32**, 975 (1974).
3. A. Gondhalekar and F. Keilmann, *Optics Commun.* **14**, 263 (1975).
4. A. Gondhalekar and E. Holzhauer, *Phys. Letters* **51A**, 178 (1975).
5. D. R. Baker, N. R. Heckenberg, and J. Meyer, *Phys. Letters* **51A**, 185 (1975).
6. A. Gondhalekar, E. Holzhauer, and N. R. Heckenberg, *Phys. Letters* **46A**, 229 (1973) and *IEEE J. Quant. Electr.* **QE-11**, 103 (1975).
7. P. Belanger and J. Boivin, *Canadian J. Phys.* **54**, 720 (1976).
8. F. R. Arams, E. W. Sard, B. J. Peyton, and F. P. Pace, *IEEE J. Quant. Electr.* **QE-3**, 484 (1967).
9. D. L. Jassby, D. R. Cohn, B. Lax, and W. Halverson, *Nucl. Fusion* **14**, 745 (1974).
10. H. R. Fetterman, B. J. Clifton, P. E. Tannenwald, and C. D. Parker, *Appl. Phys. Letters* **24**, 70 (1974) and D. Hodges, private communication.
11. T. K. Plant, L. A. Newman, E. J. Danielewicz, T. A. DeTemple, and P. D. Coleman, *IEEE Trans. Microwave Theory and Techniques* **MTT-22**, 988 (1974).
12. Z. Drozdowicz, R. J. Temkin, K. J. Button, and D. R. Cohn, *Appl. Phys. Letters* **23**, 328 (1976).
13. F. Brown, P. D. Hislop, and S. R. Kronheim, *Appl. Phys. Letters* **28**, 654 (1976).
14. A. Semet and N. C. Luhmann, Jr., *Appl. Phys. Letters* **28**, 659 (1967) and *Infrared Physics* **16**, 189 (1976).
15. D. E. Evans, L. E. Sharp, W. A. Peebles, and G. Taylor, Submitted to the *IEEE J. Quant. Electr.*
16. e.g. E. E. Salpeter, *Phys. Rev.* **122**, 1663 (1961).
17. L. Kellerer, *Z. Physik* **239**, 147 (1970).
18. D. E. Evans and P. G. Carolan, *Phys. Rev. Letters* **25**, 1605 (1970).
19. P. G. Carolan and D. E. Evans, *Plasma Phys.* **13**, 947 (1971).
20. J. Sheffield, *Plasma Phys.* **14**, 385 (1972).
21. M. Murakami and J. F. Clarke, *Nucl. Fusion* **11**, 147 (1971).
22. F. W. Perkins, Princeton Plasma Physics Laboratory Report MATT-818 (1971).
23. N. Bretz, *Applied Optics* **13**, 1134 (1974).
24. R. E. Slusher, C. M. Surko, D. R. Moler, and M. Porkolab, *Phys. Rev. Letters* **36**, 674 (1976).
25. R. Goldston, E. Mazzucato, R. Slusher, and C. Surko, Sixth IAEA Int'l Conf. on Plasma Physics and Controlled Nuclear Fusion Research, Berchtesgaden, 1976, Paper CH-35-A11.
26. R. H. Lovberg, private communication.
27. e.g. P. Belland and D. Veron, *Optics Commun.* **9**, 146 (1973).
28. D. T. Hodges, F. B. Foote, and R. D. Reel, *Appl. Phys. Letters,* Nov. 15, 1976.
29. S. M. Wolfe, K. J. Button, J. Waldman, and D. R. Cohn, *Appl. Optics,* Nov. 1976.